From a colored glass condensate to the gluon plasma: Equilibration in high energy heavy ion collisions

Jefferson Bjoraker[1,2] and Raju Venugopalan[2,3]
[1]*University of Minnesota, Department of Physics and Astronomy, 116 Church Street, Minneapolis, Minnesota 55455*
[2]*Physics Department, Brookhaven National Laboratory, Upton, New York 11973*
[3]*RIKEN-BNL Research Center, Brookhaven National Laboratory, Upton, New York 11973*
(Received 28 August 2000; published 22 January 2001)

The initial distribution of gluons at the very early times after a high-energy heavy ion collision is described by the bulk scale Q_s of gluon saturation in the nuclear wave function. The subsequent evolution of the system towards kinetic equilibrium is described by a nonlinear Landau equation for the single particle distributions [A. H. Mueller, Nucl. Phys. **B572**, 227 (2000); Phys. Lett. B **475**, 220 (2000)]. In this paper, we solve this equation numerically for the idealized initial conditions proposed by Mueller, and study the evolution of the system to equilibrium. We discuss the sensitivity of our results on the dynamical screening of collinear divergences. In a particular model of dynamical screening, the convergence to the hydrodynamic limit is seen to be rapid relative to hydrodynamic time scales. The equilibration time, the initial temperature, and the chemical potential are shown to have a strong functional dependence on the initial gluon saturation scale Q_s.

DOI: 10.1103/PhysRevC.63.024609 PACS number(s): 24.85.+p, 05.60.Cd, 05.45.−a, 52.65.Ff

I. INTRODUCTION

An outstanding problem in high-energy nuclear scattering is whether the hot and dense matter formed equilibrates to briefly form a plasma of deconfined quarks and gluons—the quark gluon plasma. This problem is of great topical interest, with collisions already taking place at the Relativistic Heavy Ion Collider (RHIC) and scheduled to take place several years hence at the Large Hadron Collider (LHC).

Whether or not a quark gluon plasma is formed depends strongly on the highly nonequilibrium initial distributions of partons formed immediately after the collision. Clearly, these distributions must influence the subsequent evolution of the system towards equilibrium. Furthermore, the problem is complicated by the rapid expansion of the system as a whole. The magnitude of the collision induced relaxation time relative to the expansion time is what determines whether equilibrium is indeed reached.

The study of equilibration in relativistic heavy ion collisions is as old as the subject itself. However, very few *ab initio* studies exist that attempt to follow the evolution of the system, all the way, from the first instants of the collision to equilibrium [1–3]. This was so because it was not known how to treat, in a self-consistent manner, the small Bjorken x ''wee'' parton modes that are responsible for particle production at central rapidities. These small x modes provide the initial conditions for the space-time evolution of the partonic matter formed in heavy ion collisions.

The occupation number of small x modes in the nuclear wave functions is large and it was shown that classical methods could be used to compute their distributions [4]. This classical effective theory is, in exact analogy to a spin glass, a color glass condensate [5,6], and is characterized by a bulk scale Q_s—the momentum scale at which gluon distributions saturate. Analytical expressions for the parton distributions were obtained in Refs. [7,8]. Subsequently, quantum corrections to the classical ''non-Abelian Weizsäcker-Williams'' fields were computed [9], and renormalization group methods [7,10] devised to study how the classical parton distributions in the nuclei changed with energy (or equivalently, with x). The scale Q_s now depends on x. This dependence is represented by a line in the x-Q^2 plane—it separates the saturated, nonlinear regime of QCD at high parton densities from that of linear QCD evolution. That Q_s is a function of x, and grows as one goes to smaller x, or equivalently, to higher energies, will only be implicit in this work.

In the classical effective field theory approach, the problem of initial conditions can be formulated as the problem of finding solutions of the Yang-Mills equation with initial conditions given by the classical fields of each of the nuclei *before* the collision [11]. Since analytical expressions exist for the classical fields of the nuclei before the collision, the initial conditions are fully determined.

Perturbative solutions of the Yang-Mills equations, which describe classical gluon production to lowest order, have been discussed by several authors [11,12]. These were found to be infrared divergent. Within the Yang-Mills approach, a fully nonperturbative treatment is therefore necessary. Nonperturbative, numerical solutions of the Yang-Mills equations have been found recently [13,14]. In particular, one now knows the initial number and energy distribution of gluons after a collision [15]. An idealized form of the initial gluon distribution, in terms of the saturation scale of the color glass condensate Q_s, was given recently Ref. [16]. These idealized distributions are sufficient for the purposes of this paper. We will reserve a more quantitative analysis using the initial distributions of Ref. [15] for a future work [17].

The initial partonic system is completely out of equilibrium. The subsequent scattering and evolution of the system towards equilibrium was studied by Mueller [16,18]. In Ref. [18], he showed that, under the assumption that the system is undergoing boost invariant expansion, the evolution of single particle distributions could be described by a nonlinear Lan-

dau equation. At very early times, this equation can be linearized,[1] and studied analytically. However, the analytical approximations soon break down, and the evolution of the system cannot be followed analytically all the way to equilibrium.

In this paper, we numerically solve the Landau equation proposed by Mueller. (Along the way, we compare our results to Mueller's analytical results and show quantitatively where the analytical approach breaks down.) We are thus able to follow the evolution of the system all the way to equilibrium. We study the dependence of the equilibration time, the initial temperature, and the chemical potential on the saturation scale Q_s of the nuclear wave function, and on α_S. (Note: one may estimate $Q_s \sim 1$ GeV at RHIC and $Q_s \sim 2-3$ GeV at LHC [16,20].) We discuss the dynamical screening of the collinear divergence arising from small angle scattering. Our results for equilibration are obtained, primarily, in a particular model of dynamical screening [21].

To conclude whether local kinetic equilibrium is attained in a system undergoing boost invariant $(1+1)$-dimensional expansion, one should compare the equilibration time $t_{\rm equil}$ to the hydrodynamic expansion time $t_{\rm hydro}$. Typically, $t_{\rm hydro} \approx R/c_0$, where R is the radius of the nucleus, and c_0 is the speed of sound in the system. For an ideal ultrarelativistic gas, $c_0 = 1/\sqrt{3}$. Our qualitative results suggest that for the energies of interest at RHIC and LHC, $t_{\rm equil} \lesssim t_{\rm hydro}$, thereby indicating that favorable conditions may exist for the formation of a hot gluon plasma at RHIC and at LHC.

In studying the likelihood of equilibration, we have only considered number conserving $2 \to 2$ processes. Naively, $2 \to 3$ processes will be suppressed by a power of α_S, and may be considered subleading. However, $2 \to 3$ processes may, in principle, be much more efficient than $2 \to 2$ processes in driving the system towards thermal equilibrium [1,22,23]. Whether this is indeed the case is a dynamical question we will not address in this work. Regardless, $2 \to 2$ processes should set an upper bound on the equilibration time. Furthermore, it is likely that the numerical techniques developed here can be adapted to quantitatively study the effects of number changing processes.

The paper is organized as follows. We begin in Sec. II by discussing the initial conditions for gluon production in nuclear collisions. After the collision, particle production is described by the space-time evolution of classical gauge fields. At late times, when the system is dilute, one can define partons, and study their interactions in a kinetic approach. The kinetic transport equation derived by Mueller is described in Sec. III. In the following section, we discuss the problem of dynamical screening of collinear divergences, and describe the particular model of screening that is employed in this work. In Sec. V, we first briefly outline the numerical method, and compare results for a linearized (Fokker-Planck) version of the Landau equation with Mueller's analytical results. We next discuss numerical results from the solution of the full Landau equation. Various measures of equilibration are described and computed as a function of the saturation scale Q_s and the coupling α_S. We summarize our results in the final section and comment on their experimental ramifications. We will also discuss the various uncertainties that need to be further quantified, and their likely impact on equilibration in high energy heavy ion collisions. An appendix contains a detailed description of the numerical method employed to solve the Landau equation.

II. THE INITIAL CONDITIONS FOR PARTON EVOLUTION

The problem of initial conditions in heavy ion collisions is as follows. Before the collision, the nucleus, as viewed in a particular gauge, is a coherent superposition of various Fock modes containing differing numbers of partons.[2] Partons in Fock modes containing a large number of partons $|qqq\cdots qgggg\cdots q\bar{q}\rangle$, have small values of x—in the language of the parton model, the momentum of the nucleus is shared among a large number of constituents. Each parton has a $+$ momentum k^+, and $x = k^+/P^+$, where P^+ is the momentum of the nucleus. The large multiplicities at central rapidities—which correspond to small x—are obtained when these small x Fock modes ''go on-shell.'' One should note that even though the small x modes carry small longitudinal momenta, their transverse momenta p_t can be large.

These small x partons are highly delocalized in the longitudinal x^- direction[3]—they have large wavelengths relative to the Lorentz contracted width of the nucleus. In addition, these virtual fluctuations are very shortlived. Any attempt to treat them in a naively classical transport approach is therefore problematic. An approach based on PQCD collinear factorization is also inadequate unless the partons also have very large transverse momenta. This is because such a picture is predicated on convolving the probabilities of parton distributions in the two nuclei with the elementary parton-parton scattering cross section. It cannot describe coherence effects which are important at small x. (For large p_t, these effects are suppressed.)

It was realized some time ago that the small x Fock states in nuclei responsible for multiparticle production at central rapidities are states of high occupation number. As a consequence, their distributions in the nuclei are described by a classical effective field theory (EFT) [4]. The classical distributions in a single nucleus can be solved and an analytical form for the distributions obtained [7,8]. The classical gluon distribution falls off as $1/k_t^2$ at large transverse momentum k_t but saturates at smaller k_t—growing only slowly as $\ln(\alpha_S \mu/k_t)/\alpha_S$. The infrared structure of the EFT is analogous to that of a spin glass in condensed matter systems [6]—it is thus a colored glass condensate [5].

The EFT approach was used in Ref. [11] to treat the problem of initial conditions in nuclear collisions. It consists of

[1] To a Fokker-Planck equation [19].

[2] For an illuminating exposition of this point of view, see Ref. [24].

[3] If P^+ is the momentum of the nucleus

solving the Yang-Mills equations in the forward light cone, after the collision, with initial conditions given by the (known) gauge fields of the nuclei before the collision.

Gluons at central rapidities are produced classically (boost invariance is assumed). Perturbative computations of the transverse momentum distributions of classically produced gluons (lowest order in α_S and lowest nontrivial order in $\alpha_S Q_s/p_t$) were first computed in Ref. [11], and later by several authors [12]. In these computations, the number distribution is found to be infrared divergent. They agree with the lowest order mini-jet predictions at large p_t.[4]

When $p_t \leqslant Q_s$, all orders in Q_s/p_t contribute equally. The perturbative computations, to lowest order in Q_s/p_t are therefore not sufficient. Thus, even at lowest order in α_S, one needs to resum all orders in Q_s/p_t. An analytic solution to this nonperturbative problem has not been found. However, the problem was recently formulated as a $(2+1)$-dimensional classical effective field theory and solved numerically [for an SU(2) gauge theory] on a two-dimensional transverse lattice [13]. The evolution of gauge fields is computed in real time, and at late times, the energy [14] and the number [15] of produced gluons at central rapidities can be computed. The initial distribution of gluons, from our numerical simulations [15], is as follows. At low values of p_t, $p_t \leqslant Q_s$ it is remarkably similar to the Bose-Einstein distribution for a gas of massive particles in two dimensions. The gluons acquire a screening mass due to strong nonlinear interactions—this also renders the distributions infrared finite. At large p_t, $p_t \gg Q_s$, the distribution is a power law Q_s^4/p_t^4. The Born-PQCD prediction for the gluon distribution is therefore obtained, as expected, in the large p_t limit.

The gluons produced at central rapidities are completely out of equilibrium. The study of the evolution of this system towards equilibrium was initiated in Refs. [16,18]. For simplicity, Mueller chose idealized initial conditions—a constant instead of a Bose-Einstein distribution for $p_t \leqslant Q_s$, and zero for $p_t \gg Q_s$—namely, the theta function $\theta(Q_s^2 - p_t^2)$. In this work, we will consider only these idealized distributions. In a later work [17], we will consider more realistic distributions computed very recently from the lattice simulations of Ref. [15]. In general, the initial spatial distribution per unit rapidity is

$$\frac{1}{L^2}\frac{dN}{d\eta} = c\,\frac{N_c^2-1}{4\pi^2\alpha_S N_c} Q_s^2, \tag{1}$$

where L^2 is the transverse area, η is the space-time rapidity, and c, determined nonperturbatively, is a weak function of $Q_s R$. For an SU(2) gauge theory, it was computed recently in Ref. [15] to be $c = 1.29 \pm 0.09$ in the regime of interest.

The initial distributions are highly anisotropic, with the produced partons having zero longitudinal momentum p_z. Assuming boost invariance, and using the relation

$$f(x,p) = \frac{(2\pi)^3}{2(N_c^2-1)}\,\frac{dN}{d^3p\,d^3x}, \tag{2}$$

for the single particle distribution $f(x,p)$, one finds at late times that[5]

$$f(x,p) = \frac{c}{\alpha_S N_c}\,\frac{1}{t}\,\delta(p_z)\,\theta(Q_s^2 - p_t^2). \tag{3}$$

At late times, the occupation number of partons in the transverse plane becomes small, and their evolution can no longer be followed on the lattice. However, when the occupation number is not too large, transport theory can be applied to study the further evolution of the system. The initial condition for this evolution is given by the single particle distribution in Eq. (3).

Using the results of Ref. [14], which determined the time at which gluons come on-shell after a collision, we can estimate the time at which small angle scattering between the gluons can be described by the Boltzmann equation. The formation times, using $Q_s = 1$ GeV for RHIC and $Q_s = 2$–3 GeV for LHC, are

$$t_i \sim 1.40\ \text{GeV}^{-1} \text{ for RHIC}, \quad t_i \sim 0.62\ \text{GeV}^{-1} \text{ for LHC}. \tag{4}$$

Next, we suppose that a transport theory based treatment of gluon scattering is applicable when the gluon occupation number is less than unity. Letting $d\eta$ be $d\eta = dz/t_i = 1$ or $dz = t_i$, and using, $dN/d^3x d^3k$ from Ref. [18] at $z=0$, we find

$$t_0 = \frac{c}{\alpha_S N_c}\,t_i. \tag{5}$$

Here $t_0 > t_i$ is the time where the gluon occupation number is dilute enough that their subsequent interactions can be described as the small angle scattering of on-shell gluons.

III. THE LANDAU TRANSPORT EQUATION

At times $t > t_0$, where t_0 was defined in Eq. (5), a Boltzmann-like transport equation is appropriate for describing the late-time evolution of the highly anisotropic initial gluon distribution discussed in the previous section. We will show below that, for central high-energy heavy ion collisions, assuming boost invariance, the transport equation reduces to a Landau-type transport equation [19].

In the problem of interest, the typical scale of spatial variations is large compared to the typical scale of gluon-gluon scattering. The evolution of the system can therefore be described by a local Boltzmann-like kinetic equation for the single particle gluon distribution $f(x,p,t)$, which gives

[4]For detailed comparisons, see the papers by Gyulassy and McLerran, and by Guo, in Ref. [12].

[5]The δ-function distribution is of order $1/\Delta p_z$. We shall see later, from the early time analytical solution of the Fokker-Planck equation, that the longitudinal momentum changes little in the time in takes for the occupation number to decrease below unity.

the density of excitations of momentum $\vec{p}$ at a point $(\vec{x},t)$. The Boltzmann equation is

$$\frac{\partial f}{\partial t}+\vec{v}\cdot\vec{\nabla}f=C(f), \tag{6}$$

where $C(f)$ is the collision integral which represents the change, due to collisions, per unit time, in the number of particles per unit phase space volume.

Let us first consider the left-hand side of the above equation. We will assume that the transverse dimensions of the collision volume in central heavy ion collisions are sufficiently large that the initial expansion of the system is one-dimensional. The distribution f then only depends on z, the coordinate corresponding to the collision axis. Since it is independent of the transverse coordinate x_t, Eq. (6) has the form

$$\frac{\partial f(\vec{p},z,t)}{\partial t}+v_{p_z}\frac{\partial f(\vec{p},z,t)}{dz}=C[f(\vec{p},z,t)], \tag{7}$$

where $v_{p_z}=p_z/|\vec{p}|$. A further simplification follows from the assumption that the central rapidity region is approximately Lorentz invariant under boosts [25]. As was pointed out by Baym many years ago [26], this assumption greatly simplifies the problem of solving Eq. (7) since it relates the distribution function at different z's in the central region. It therefore suffices to compute f in the zero-rapidity slice alone. Because f is a scalar under Lorentz transformations, it satisfies the relation

$$f(p_t,p_z,z,t)=f(p_t,p_z',t). \tag{8}$$

Here $p_z'=\gamma(p_z-up)$, the transformation velocity $u=z/t$, and $\gamma=(1-u)^{-1/2}=t/\tau$, where the proper time $\tau=\sqrt{t^2-z^2}$.

Computing $\partial f/\partial z$ using Eq. (7), the Lorentz transformation relation, $\partial\tau/\partial z|_{z=0}=0$, and $\partial p_z'/\partial z|_{z=0}=-p/t$, one finds [26] at $z=0$,

$$v_{p_z}\frac{\partial f}{\partial z}=-\frac{p_z}{t}\frac{\partial f}{\partial p_z}. \tag{9}$$

The Boltzmann equation now reduces to

$$\left.\frac{\partial f(p_t,p_z,t)}{\partial t}\right|_{p_z t}\equiv\left(\frac{\partial}{\partial t}-\frac{p_z}{t}\frac{\partial}{\partial p_z}\right)f(p_t,p_z,t)$$
$$=C[f(p_t,p_z,t)]. \tag{10}$$

Note that, as a consequence of our manipulations, assuming uniform distributions in the transverse direction and boost invariance in the longitudinal direction, the single particle distribution $f(x,p,t)$ is now expressed as a function of $\vec{p}$ and t alone. The kinetic equation above, in the absence of collisions, has the free streaming solution for f [26], namely,

$$f(t,p)=\exp(-\beta_0\sqrt{p_\perp^2+p_z^2t^2/\gamma_0^2}), \tag{11}$$

where β_0 and γ_0 are constants.

We shall now consider the collision term $C[f]$ on the right-hand side of the above equation. If we assume that the changes in momentum q in a collision are small, namely, $q/Q_s\ll 1$, we can treat the collision integral as simple diffusion in momentum space. Following the discussion in Lifshitz and Pitaevskii [19], one can write

$$C[f]=-\frac{\partial s_\alpha}{\partial p_\alpha}, \tag{12}$$

where the flux

$$s_\alpha=\left(\frac{\alpha N_c}{\pi}\right)^2\mathcal{L}\int d^3\vec{p}\left(f\frac{\partial f'}{\partial\vec{p}_\beta'}-f'\frac{\partial f}{\partial\vec{p}_\beta}\right)$$
$$\times[\delta_{\alpha\beta}(1-\vec{v}\cdot\vec{v}')+v_\alpha v_\beta'+v_\beta v_\alpha']. \tag{13}$$

Note that $\vec{v}=\vec{p}/|\vec{p}|$.

We have used in Eq. (13) the cross section for gluon-gluon elastic scattering, which in the limit of small momentum transfer squared $q^2=-\hat{t}$, is

$$\frac{d\sigma}{d\hat{t}}=-\left(\frac{\alpha_S N_c}{\pi}\right)^2\frac{(2\pi)^3}{2(N_c^2-1)}\frac{1}{\hat{t}^2}. \tag{14}$$

The collision integral contains a logarithmic collinear divergence arising from small angle scattering. It is represented here by $\mathcal{L}$, defined as

$$\mathcal{L}=\int_{q_{\min}}^{q_{\max}}\frac{dq}{q}. \tag{15}$$

The minimal momentum transfer is $q_{\min}=Q_s\theta_{\min}$, where $\theta_{\min}$ is the minimum scattering angle. Also, $q_{\max}$ is the maximum momentum transfer. How one may determine $q_{\min}$ and $q_{\max}$ is discussed in the next section.

Having started from Eq. (6), combining Eqs. (10) and (13), we arrive at the considerably simpler expression, the Landau equation [19,27]

$$\frac{\partial f}{\partial t}-\frac{p_z}{t}\frac{\partial f}{\partial p_z}=\lambda n\mathcal{L}\nabla_{\vec{p}}^2 f+2\lambda n_{-1}\mathcal{L}\nabla_{\vec{p}}\cdot(\vec{v}f), \tag{16}$$

with the definitions

$$n(t)=g_G\int\frac{d^3p}{(2\pi)^3}f(t,\vec{p}),$$

$$n_{-1}(t)=g_G\int\frac{d^3p}{(2\pi)^3}\frac{f(t,\vec{p})}{|\vec{p}|},$$

$$\lambda=2\pi\alpha_S^2\frac{N_c^2}{N_c^2-1}. \tag{17}$$

Here, $g_G=2(N_c^2-1)$ and $\nabla_{\vec{p}}$ refers to differentiation with respect to $\vec{p}$.

Multiplying both sides of Eq. (16) by d^3p and integrating, one finds

$$\frac{d}{dt}(tn)=0, \tag{18}$$

namely, the number density of gluons has the behavior $n \propto 1/t$. Taking the second moment of Eq. (16), one finds the following exact relation in the central region [26]:

$$\frac{\partial \epsilon}{\partial t}+\frac{(\epsilon+P_L)}{t}=0, \tag{19}$$

where the local energy density is given by

$$\epsilon(t)=g_G\int \frac{d^3p}{(2\pi)^3}pf(p,t), \tag{20}$$

and the longitudinal pressure is

$$P_L(t)=g_G\int \frac{d^3p}{(2\pi)^3}\frac{p_z^2}{p}f(p,t). \tag{21}$$

In the hydrodynamic regime where $P_L=\epsilon/3$, the ideal gas equation of state gives $\epsilon \sim t^{-4/3}$. We will return to a discussion of these quantities later on in the paper.

It is convenient to define the quantities $\eta=tn$ and $\eta_{-1}=tn_{-1}$. The Landau equation can thus be rewritten as

$$t\frac{\partial f(t,\vec{p})}{\partial t}-p_z\frac{\partial f(t,\vec{p})}{\partial p_z}=\lambda\,\eta\mathcal{L}\nabla_p^2 f(t,\vec{p}) + 2\lambda\,\eta_{-1}(t)\mathcal{L}\nabla_{\vec{p}}\cdot[\vec{v}f(t,\vec{p})]. \tag{22}$$

If η_{-1} is taken to be independent of time, this equation is the Fokker-Planck equation: the coefficient of the first term would be the diffusion coefficient, while that of the second would be the coefficient of friction.

IV. SCREENING OF COLLINEAR DIVERGENCES IN THE LANDAU TRANSPORT EQUATION

In the one gluon exchange approximation, as in Coulomb scattering, the transport integral in Eq. (13) has a logarithmic collinear divergence—represented by $\mathcal{L}$. In Ref. [16], the condition applied at early times was that in the maximal distance $1/q_{\min}$ corresponding to the minimal momentum transfer $q_{\min}$, one has at most one scattering.[6] From this condition, by using the initial gluon distribution, Mueller finds at the earliest times that

$$M_m^2=\left(\frac{c\alpha_S N_c}{\pi}\right)^{2/3}\frac{Q_s^2}{(Q_s t)^{2/3}}. \tag{23}$$

A more general expression, for any arbitrary number density, is easily derived to be

$$M_m^2=\left[\left(\frac{\alpha_S N_c}{\pi}\right)^2\frac{(2\pi)^3}{2(N_c^2-1)}n(t)\right]^{2/3}. \tag{24}$$

Alternately, one can use the more conventional prescription of regulating the logarithmic collinear divergence in $\mathcal{L}$ through the exchange of dressed gluons characterized by a Debye screening mass. A kinetic theory expression for the Debye screening mass can be derived from the screening of a timelike gluon propagator in a medium of gluon excitations [21]. One obtains

$$m_D^2=-\frac{\alpha_S N_c}{\pi^2}\lim_{|\vec{q}|\to 0}\int d^3p\frac{|\vec{p}|}{\vec{q}\cdot\vec{p}}\vec{q}\cdot\vec{\nabla}_{\vec{p}}f(t,\vec{p}). \tag{25}$$

One can check that for an equilibrium Bose distribution, one recovers the standard result: $m_D^2=4\pi\alpha_S N_c T^2/3$. For our initial conditions, it is the screening of the longitudinal gluons in the transverse direction that is relevant. Performing an integration by parts, this transverse Debye mass is given by the expression [28]

$$m_T^2=\frac{\alpha_S N_c}{\pi^2}\int\frac{d^3p}{|\vec{p}|}f(p). \tag{26}$$

At the very early stage of the $2\to 2$ scattering, the expression in Eq. (26) is, in principle, less reliable since the system is completely out of equilibrium. However, at later times, as the system approaches equilibrium, m_D should be more reliable. One could attempt to parametrize the infrared cutoff of small angle scattering such that it interpolates between the two limits. However, at present there is no theoretical justification of any particular form. Since collisions become more frequent as one approaches equilibrium, it is likely that the Debye mass is a more reliable cutoff to use. At any rate, it is important that one at least have the right limit as the system approaches equilibrium.

In Refs. [16,18], the value of $q_{\max}$ is held fixed at early times. This is because if one rewrites $\mathcal{L}$ in Eq. (15) as

$$\mathcal{L}=\ln\left(\frac{\langle p_t\rangle}{m_T}\right), \tag{27}$$

it is argued, on the basis of analytical approximations to Eq. (31) below, that $\langle p_t\rangle/Q_s$ changes appreciably only over a long time scale ($t\sim e^{1/\sqrt{\alpha_S}}$). Since the Debye mass has a stronger time dependence, $\mathcal{L}$ grows with time. On account of the approximations made in arriving at this conclusion, it is useful to check whether this behavior of $\mathcal{L}$ is obtained by computing $\langle p_t\rangle$ and m_T self-consistently at each step in our

[6]This condition satisfies the requirement that the soft field (due to all the other hard gluons) that a particular hard gluon scatters off be at most of size $1/g$. This is so because the freed gluons come from the saturated component of the nuclear wave function of size $1/g$—see the discussion in Sec. II.

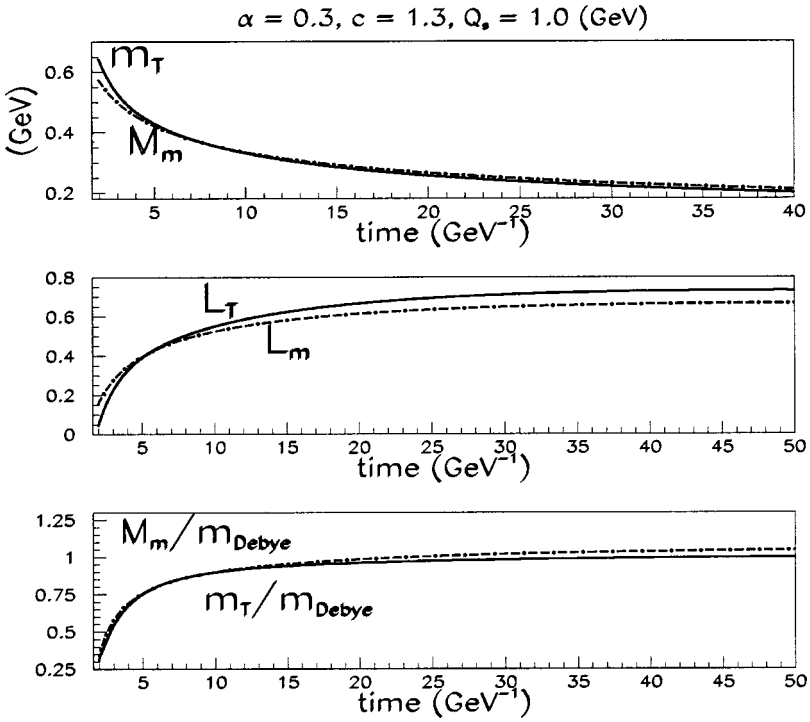

FIG. 1. The dynamical screening masses, M_m from Eq. (24) obtained from Ref. [16] and the m_{T} from Eq. (26) obtained from linear response theory [21] plotted as functions of time in GeV^{-1} units. Also plotted versus time are the logarithms $\mathcal{L}_m$ and $\mathcal{L}_t$ obtained by combining Eqs. (24) and (26), respectively, with Eq. (27).

numerical simulations.[7] We indeed do find, as shown in Fig. 1, that $\mathcal{L}$ grows rapidly initially as a function of time but levels out to a constant as the system approaches equilibrium.

In Fig. 1, we plot the infrared masses in Eqs. (24) and (26), as well as the corresponding contribution $\mathcal{L}$ to the collision integral, as a function of time (in units of $1/Q_s$). One sees that while the relative difference at early times is large, it is much less so at later times. We have also solved the transport equation using both cutoffs. While there is some quantitative difference between the two, they do not affect our qualitative conclusions. For the rest of this work, we will therefore use the Debye mass in Eq. (26).

Debye screening occurs due to the exchange of longitudinal gluons. One may worry whether the screening of transverse gluons will introduce an additional scale since the static magnetic mass is parametrically larger than the Debye mass. However, the conventional wisdom is that, for transport cross sections, magnetic screening is also cut off in the infrared by the Debye mass [29,30]. The same, for instance, is not true of color transport—the color conductivity is regulated by a magnetic mass of order g^2T [31]. The dynamical screening of infrared divergences in $2\rightarrow n$ $(n\geqslant 2)$ transport cross sections merits further study.

V. RESULTS FROM NUMERICAL SOLUTION OF THE FOKKER-PLANCK EQUATION

We will first consider, as a ''warmup exercise,'' the solution of Eq. (22) for the case where η_{-1} is held constant. The Landau equation then reduces to the Fokker-Planck equation. To check the consistency of our numerical simulation, we will compare, in detail, the numerical solution of the Fokker-Planck equation to the early time analytical solution found in Refs. [16,18]. We will discuss solutions to the nonlinear Landau equations in the next section.

We first define $\tilde{f}=tf$, $\mathcal{L}=\frac{1}{3}\ln(t/t_0)\equiv\frac{1}{3}\xi$, where t_0 is a constant defined in Eq. (5). (As discussed in the previous section, this assumption is justified at early times.) Scaling $\lambda/3\rightarrow\lambda$, we can rewrite Eq. (22) as

$$\left(\frac{\partial}{\partial\xi}-\frac{\partial}{\partial p_z}p_z\right)\tilde{f}=\lambda\,\eta\xi\nabla_{\vec{p}}^2\tilde{f}+2\lambda\,\eta_{-1}\xi\nabla_{\vec{p}}\cdot(\vec{v}\tilde{f}). \quad (28)$$

Equation (28) is a Fokker-Planck equation if η_{-1} is held fixed. If one integrates Eq. (28) with respect to d^3p, $d^3pp_\perp^2$ and $d^3pp_z^2$ we obtain Eqs. (17), (18), and and (19) in Ref. [18],

$$\frac{d}{d\xi}\eta=0, \quad (29)$$

$$\frac{d}{d\xi}\langle p_z^2\rangle+2\langle p_z^2\rangle=2\lambda\,\eta\xi-\frac{\lambda\,\eta_{-1}\xi}{\eta}\tilde{P}_L(\xi), \quad (30)$$

and

$$\frac{d}{d\xi}\langle p_\perp^2\rangle=4\lambda\,\eta\xi\left(1-\frac{\eta_{-1}\eta_{+1}}{\eta^2}\right)+\frac{\lambda\,\eta_{-1}\xi}{\eta}\tilde{P}_L(\xi), \quad (31)$$

where $\tilde{P}_L=tP_L$ is defined by Eq. (21). These equations are exact. We can therefore perform the following consistency check on our solution. With the initial conditions in Eq. (3) and the boundary condition that $f(p_x,p_y,p_z,t)=0$ if any

[7]We thank A. Dumitru for discussions on this point.

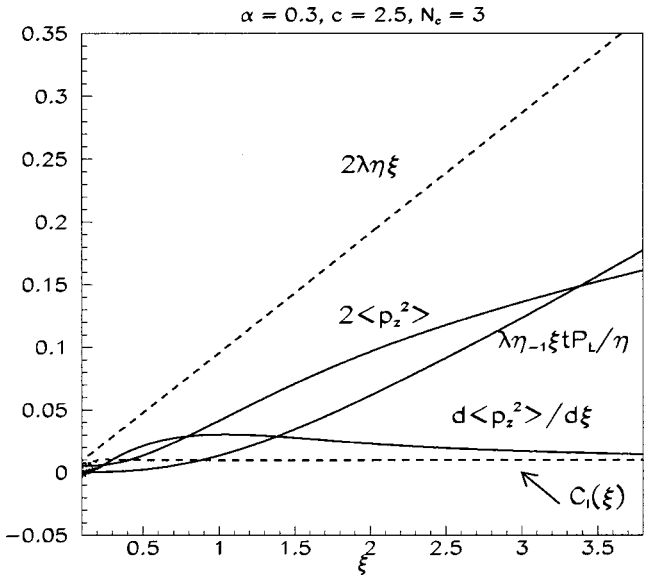

FIG. 2. Numerical solution to the Boltzmann equation with constant η_{-1} where each term in Eq. (34) is plotted as a function of $\xi=\ln(t/t_0)$.

p_x, p_y or $p_z\rightarrow\infty$, we numerically determine f for all time, directly compute $\langle p_\perp^2\rangle$ and $\langle p_y^2\rangle$, and check to see if Eqs. (29)–(31) are satisfied. Mueller supposes that at early times the first term on the left-hand side and the last term on the right-hand side of Eq. (30) are small, thereby yielding the solution

$$\langle p_z^2\rangle=\lambda\,\eta\xi. \tag{32}$$

It is demonstrated in Fig. 2 that this approximation, in practice, is not a very good one. At very early times, if $\xi\sim 0$ we see that the first term on the LHS of Eq. (30) is of the same order as the remaining terms. We cannot therefore ignore it. We can ignore the term proportional to $\tilde{P}_L(t)$ in Eq. (30) for early times. Then Eq. (30) becomes

$$\frac{d}{d\xi}\langle p_z^2\rangle+2\langle p_z^2\rangle=2\lambda\,\eta\xi.$$

Its solution is

$$\langle p_z^2\rangle=\lambda\,\eta\xi+\frac{\lambda\,\eta}{2}[\exp(-2\xi)-1]. \tag{33}$$

This solution (see Fig. 4) agrees much better with the numerical results than Eq. (32) does. We define $C_I(\xi)$ as

$$2\lambda\,\eta\xi-\frac{\lambda\,\eta_{-1}\xi}{\eta}\tilde{P}_L(\xi)-\frac{d}{d\xi}\langle p_z^2\rangle-2\langle p_z^2\rangle=C_I(\xi), \tag{34}$$

where $C_I(\xi)$ should be small if Eq. (30) is satisfied. Figure 2 verifies indeed that this is so.

Next, look at Eq. (31). If we assume that both η_{-1} and η_{+1} are constant with respect to time and determined by the initial condition, Eq. (3),

$$\eta=c\,\frac{N_c^2-1}{4\pi^2\alpha_S N_c}Q_s^2,\qquad \eta_{-1}=c\,\frac{N_c^2-1}{2\pi^2\alpha_S N_c}Q_s,$$

$$\eta_{+1}=c\,\frac{N_c^2-1}{6\pi^2\alpha_S N_c}Q_s^3. \tag{35}$$

Using Eq. (35) we rewrite Eq. (31) as

$$\frac{d}{d\xi}\langle p_\perp^2\rangle=-\frac{4}{3}\lambda\,\eta\xi+\frac{\lambda\,\eta_{-1}\xi}{\eta}\tilde{P}_L(\xi). \tag{36}$$

Again the term containing $\tilde{P}_L$ is small. We therefore solve the equation above, with the appropriate boundary conditions, to find

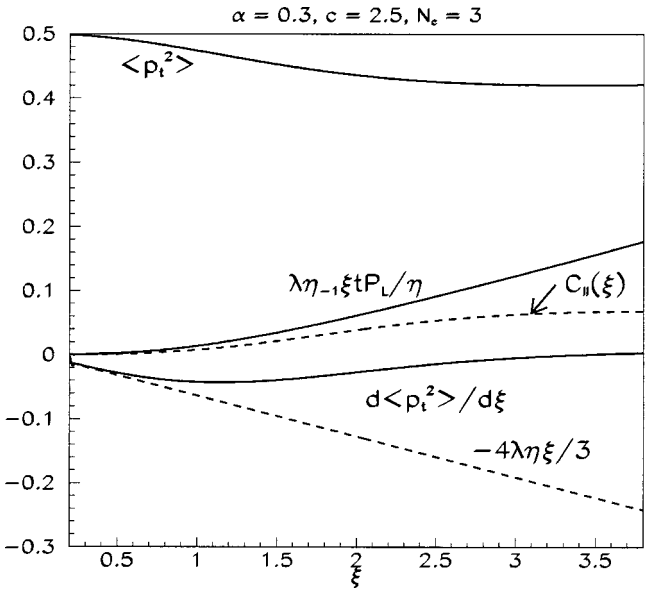

FIG. 3. Each term in Eq. (38) plotted as a function of $\xi=\ln(t/t_0)$.

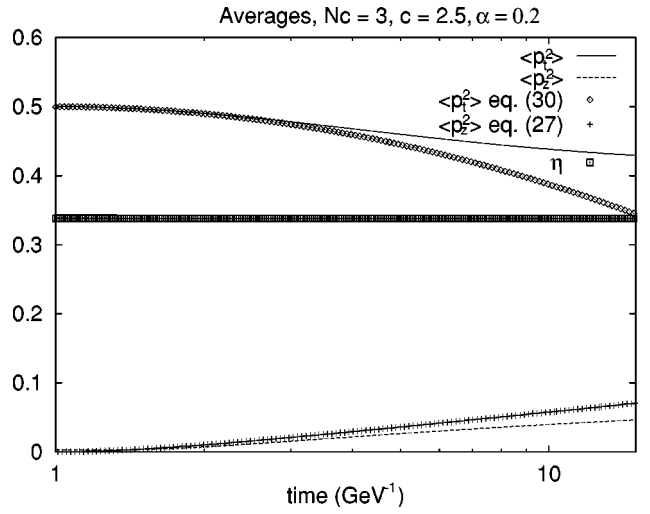

FIG. 4. Numerical results for $\langle p_z^2\rangle$ and $\langle p_\perp^2\rangle$, plotted as a function of time, compared with the analytical approximations in Eqs. (33) and (37) . Also plotted is η as a function of time.

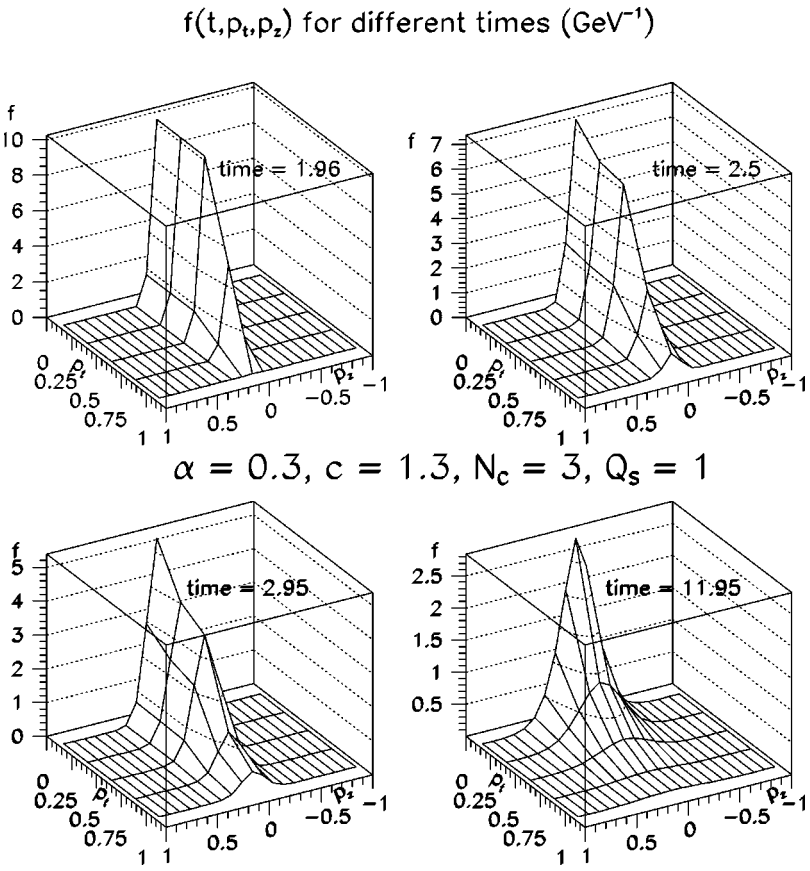

FIG. 5. The number of gluons per unit of phase space $f(t,\vec{p})$ plotted as a function of $p_\perp$ and p_z for different times. $N_c=1$, $\alpha_S=0.3$, $c=1.3$ and $Q_s=1$ GeV. Units of time are in GeV^{-1}.

$$\langle p_\perp^2\rangle = \frac{Q_s^2}{2} - \frac{2}{3}\lambda\,\eta\xi^2. \tag{37}$$

As previously, define $C_{II}(\xi)$ such that

$$\frac{d}{d\xi}\langle p_\perp^2\rangle + \frac{4}{3}\lambda\,\eta\xi - \frac{\lambda\,\eta_{-1}\xi}{\eta}\tilde{P}_L(\xi) = C_{II}(\xi). \tag{38}$$

Figure 3 verifies that Eq. (38) is satisfied for early times.

Finally, we check to see how well Eq. (29) is satisfied numerically. Figure 4 plots the numerical result for η vs t and demonstrates that η is constant with respect to t. As discussed earlier, Fig. 4 also compares the numerical result for $\langle p_z^2\rangle$ and $\langle p_\perp^2\rangle$ with the analytical solutions of Eqs. (36) and (30) given by Eqs. (33) and (37).

VI. RESULTS FROM NUMERICAL SOLUTION OF THE LANDAU TRANSPORT EQUATION

In the previous section, we numerically solved the Boltzmann equation using Mueller's approximation for the minimum scattering angle, and with η_{-1} fixed for all time [Eq. (28)].[8] Since the previous analysis is only expected to be valid for early times, one must solve the general expression (22) with η_{-1} determined self-consistently.

In this section, we will discuss results from numerical solutions of the Landau equation in Eq. (22) employing the initial single particle distribution given by Eq. (3) and the dynamical screening mass given by Eq. (26). The equation is a second order partial integrodifferential equation. It can be solved by combining the alternating direction implicit (ADI) method and the Crank-Nicholson differencing scheme [32,33]. A detailed discussion of the numerical procedure can be found in the Appendix.

We will first begin by briefly describing the evolution of the single particle distribution and its moments. Next, we will discuss various measures of kinetic equilibration and hydrodynamic flow for a system undergoing boost-invariant one-dimensional expansion. Finally, we will discuss our numerical results for these quantities for different values of Q_s and α_S.[9]

A. Single particle distributions

The initial distribution for the numerical solution of Eq. (22) is given by Eq. (3), at the initial time, determined from Ref. [14], given by Eq. (4). The time evolution of the single particle distribution $f(t,p_z,p_\perp)$ is shown in Fig. 5 for a particular set of initial parameters. It begins its time evolution as a delta function in p_z (represented practically by a narrow Gaussian distribution) and as a step function in $p_\perp$ — see Eq.

[8]Recall that η_{-1} is an integral representing the ''-1'' moment of f.

[9]We will ignore running coupling effects in this analysis. It is argued in Ref. [18] that running coupling effects in the evolution are $O(\sqrt{\alpha_S})$ and therefore suppressed.

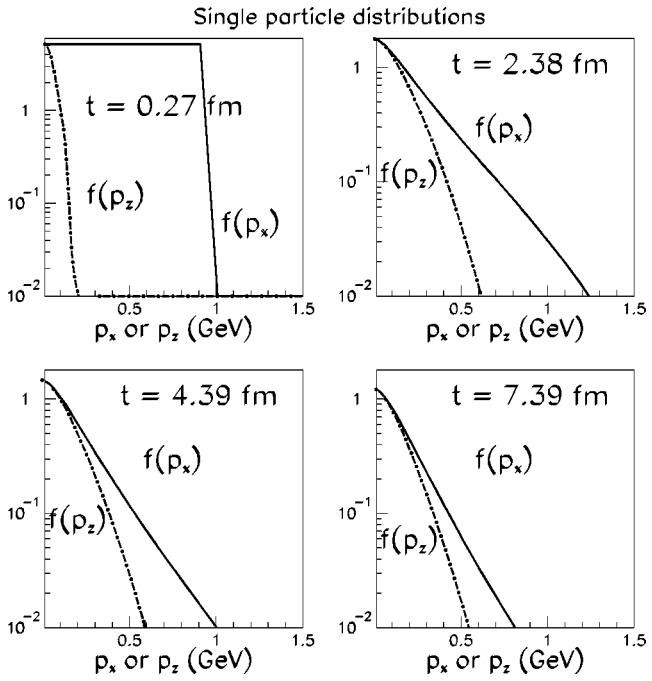

FIG. 6. The single particle distributions, for fixed p_x or p_z plotted as a function of p_z and p_x, respectively, for different times in the evolution of the distribution. The results are for $\alpha_S=0.3$, $Q_s=1$, $c=1.3$, and $N_c=3$.

(3). As time proceeds, we see the $p_\perp$ modes get scattered off the transverse plane in the longitudinal direction. The larger $p_\perp$ modes decrease rapidly as the p_z distribution widens out. At about $t=11.95$ GeV^{-1}, the p_z distribution is at its broadest extent.

The behavior of the single particle distributions are seen more clearly in Fig. 6, where we have plotted f, as a function of p_z or p_x, for fixed p_x and p_z, respectively. We see initially that the two distributions are widely different. As time proceeds, they converge relatively rapidly at soft momentum but much more slowly in the tails. If thermal equilibrium is defined strictly as the distributions being completely isotropic, this condition is reached only asymptotically, if at all.

Figure 7 shows, for particular initial parameters, the averages $\langle p_x^2\rangle$, $\langle p_y^2\rangle$, and $\langle p_z^2\rangle$ as functions of time. $\langle p_z^2\rangle$ starts at zero and quickly rises before converging slowly to $\langle p_x^2\rangle$ and $\langle p_y^2\rangle$, which, in turn, decrease monotonically with time. The nontrivial behavior of $\langle p_z^2\rangle$ is because the system is undergoing longitudinal expansion. In a box at rest, one expects that $\langle p_z^2\rangle$ will show more of a monotonic behavior before leveling off. It again appears from Fig. 7 that the convergence to isotropic distributions is very slow. This is particularly so since the second moment of the distribution weights the high momentum tail unduly. The latter, as we observed in Fig. 6, takes longer to equilibrate.

Interestingly, as we will discuss in the following, the convergence of bulk thermodynamic observables to the expected equilibrium values is much more rapid. A likely explanation is that these observables are much less sensitive to the high momentum tail of the distribution.

B. Kinetic equilibrium and hydrodynamics

From Figs. 6 and 7, it appears that the distribution, as a whole, become isotropic only asymptotically. This statement is particularly true of the tails, in p_z and p_t, of the distributions. The distributions agree more closely at softer momenta. Nevertheless, as we shall discuss below, when we look at thermodynamic signatures of equilibrium, they converge relatively rapidly to the expected behavior in a fluid undergoing boost-invariant one-dimensional expansion.

Let us first discuss what this expected behavior is. Since we only consider $2\rightarrow 2$ processes in this work, the total num-

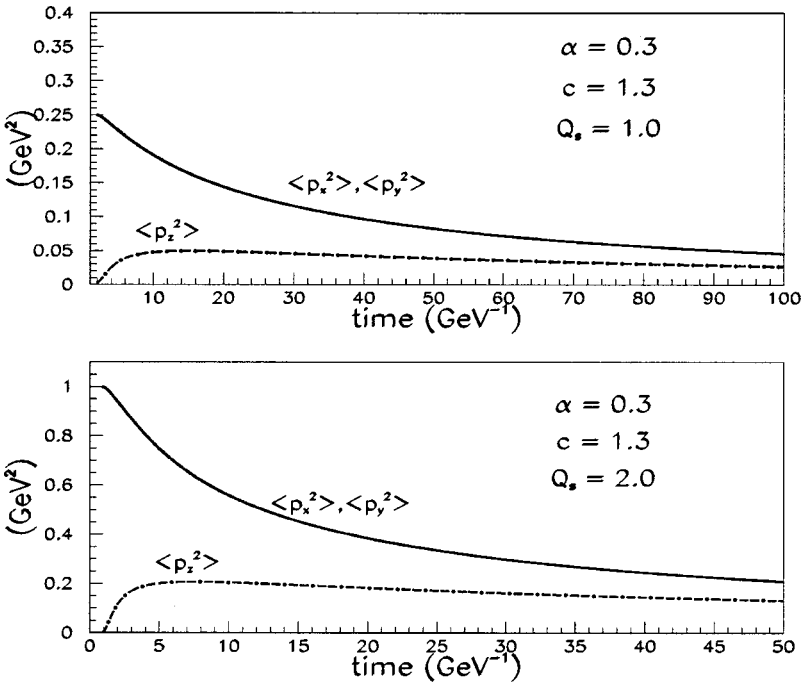

FIG. 7. The averages $\langle p_x^2\rangle$, $\langle p_y^2\rangle$, and $\langle p_z^2\rangle$ versus time in GeV^{-1} units for different values of α_S, c, and Q_s. In all cases, $N_c=3$.

ber of gluons is fixed. The equilibrium solution of the classical Boltzmann equation, Eq. (22), thus has the form

$$f(t,p)=\exp\{\beta(t)[\mu(t)-p]\}. \tag{39}$$

Here $\mu(t)$ is the chemical potential, and $\beta(t)=1/T(t)$, where T is is the temperature. Substituting this equilibrium distribution in Eq. (17), one obtains

$$n(t)=2\frac{(N_c^2-1)}{\pi^2}T^3(t)\exp\left(\frac{\mu}{T}\right), \quad n_{-1}(t)$$

$$=\frac{(N_c^2-1)}{\pi^2}T^2(t)\exp\left(\frac{\mu}{T}\right). \tag{40}$$

The average energy density is defined to be

$$\epsilon(t)=g_G\int\frac{d^3p}{(2\pi)^3}|\vec{p}|f(t,p). \tag{41}$$

From Eq. (41) and Eq. (40), the energy per particle at equilibrium is

$$E(t)=\epsilon(t)/n(t)=3T(t). \tag{42}$$

Now, the entropy density of a classical Boltzmann gas is defined as

$$s(t)=-g_G\int\frac{d^3p}{(2\pi)^3}f\ln f. \tag{43}$$

In equilibrium, the entropy per particle is simply

$$S(t)=\frac{s(t)}{n(t)}=3-\frac{\mu}{T}. \tag{44}$$

We noted previously, since the number of gluons is conserved, that $tn(t)=$const. Also note that, since the entropy per particle is constant in equilibrium, we find from the above equation that $\mu/T=$const. From these constraints, the system in equilibrium must satisfy

$$T^3t=\text{const}, \quad \epsilon t^{4/3}=\text{const}. \tag{45}$$

Finally, recall we had defined the longitudinal pressure in the central slice in Eq. (21) as

$$P_L(t)=g_G\int\frac{d^3p}{(2\pi)^3}\frac{p_z^2}{p}f(p,t).$$

One can similarly define the transverse pressure P_T to be

$$P_T(t)=g_G\int\frac{d^3p}{(2\pi)^3}\frac{p_t^2}{2p}f(p,t). \tag{46}$$

From Eq. (19), and the above relations, the condition for ideal hydrodynamics is

$$P_T=P_L=\frac{1}{3}\epsilon. \tag{47}$$

The approach to equilibrium, in the sense of ''saturating'' the above thermodynamic (and hydrodynamic) identities, has been studied, in the relaxation time approximation, by several authors [26,34,35]. This approximation is also employed in studies with minijet initial conditions [36,28]. The collision kernel in Eq. (10) can be written formally as [27,37]

$$C[f(p_z,p_t,t)]=-\frac{(f-f_{\text{equil}})}{\theta}, \tag{48}$$

where θ, the collision or relaxation time, is in general a function of time and momentum. The relaxation time approximation is one where the momentum dependence of θ is neglected. Baym studied equilibration in this approximation taking θ to be a constant. He showed that the thermodynamic relations in Eqs. (45) and (47) were satisfied only asymptotically in time.[10] Nevertheless, the convergence of the system to the asymptotic value is rapid. The system, while not quite in local thermodynamic equilibrium, is sufficiently close to it that equilibrium is a good working assumption. Subsequently, Gavin studied equilibration in the relaxation time approximation assuming θ to have the time dependence [34]; $\theta=\alpha t$, where α is a constant. Depending on the value of α, the system approaches the hydrodynamic limit quickly (smaller α's) or free streaming (larger α's). Heiselberg and Wang [35], studied the general case, $\theta=t^p$. They conclude that for $p<1$ thermalization is attained, while the system free streams for $p>1$. The case $p=1$ studied by Gavin is the marginal one, interpolating between the two regimes for different α's. In a subsequent paper [38], Heiselberg and Wang study the dependence of θ in finite temperature QCD, and tentatively conclude that $p\sim 1/3<1$.

C. Convergence to the hydrodynamic limit

In this work, as discussed in Sec. III, we go beyond the relaxation time approximation in treating the collision kernel. It is not necessary therefore, once a screening mechanism is postulated, to specify the time dependence of the collision time. In the following, we will discuss our results for the thermodynamic relations stated in the previous section.

In Fig. 8 we show the entropy per particle S plotted as a function of time. As shown for typical values of α_S, c, and Q_s, it initially increases rapidly and flattens out, monotonically approaching its asymptotic value (thereby implying that μ/T goes to a constant as well). The expression in Eq. (43), used in the computation of Fig. 8, is the correct one, except at very early times when the well-known full expression for the entropy density of a Bose gas should be used. Thus, where the result in Fig. 8 is going to zero is where the classical Boltzmann expression for the entropy density is breaking down. We have checked that the full expression ensures that the entropy per particle is always positive definite. The triangles in Fig. 8 correspond to the entropy per particle as-

[10]This is indeed what we would conclude from our study of the single particle distributions in the previous subsection.

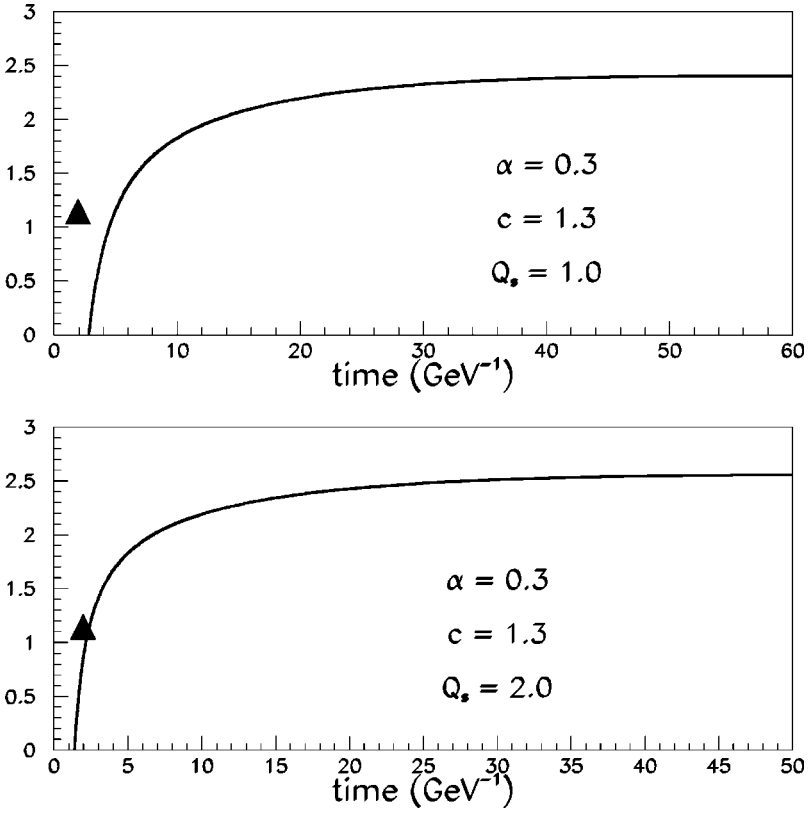

FIG. 8. The entropy per particle S plotted as a function of time for $\alpha_S=0.3$, $c=1.3$, and $Q_s=1$ (GeV). In both cases, $N_c=3$. The triangles denote the entropy per particle of a two-dimensional Boltzmann gas.

suming the partons are initially localized on the two-dimensional transverse plane.

The convergence of other thermodynamic quantities to the hydrodynamic limit is shown in Fig. 9. Again, we note that the convergence to their asymptotic values is much more rapid than one would expect by looking at the single particle distributions alone. Our results suggest that the collision time effectively has a time dependence t^p with $p<1$.

Since the convergence to the hydrodynamic limit is only asymptotic, deciding when the system can be described in terms of thermodynamic quantities is somewhat subjective. Here, we define the equilibrium time $t_{\rm eq}$ as the time it takes

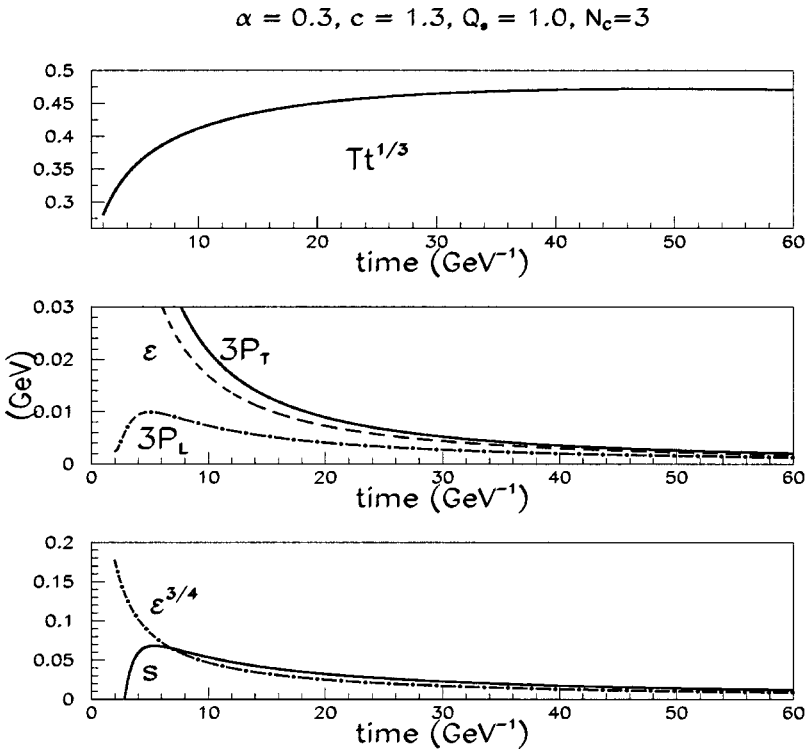

FIG. 9. The top panel plots $Tt^{1/3}=(\epsilon/3n)t^{1/3}$ where ϵ is the energy density and n the number density; the middle panel the ϵ, the longitudinal pressure P_L and the transverse pressure P_T; the bottom panel $\epsilon^{3/4}$ and the entropy density s; all plotted versus time in GeV^{-1} units, for typical values of α_S, c, Q_s, and N_c.

TABLE I. Equilibration times, temperatures and chemical potentials as a function of α_S and Q_s for $c=1.3$, and $N_c=3$.

α_S	Q_s(GeV)	$t_{\rm eq}$(fm)	$T_{\rm eq}$(MeV)	μ(MeV)
0.1	1.0	12.24 ± 1.92	171.05 ± 4.9	137.78 ± 19.3
0.2	1.0	5.8 ± 0.83	166.28 ± 5.19	144.71 ± 15.22
0.2	2.0	4.48 ± 0.75	304.32 ± 19.39	212.95 ± 31.23
0.3	1.0	3.24 ± 0.44	174.27 ± 5.21	157.86 ± 16.18
0.3	1.4	2.77 ± 0.60	234.70 ± 11.60	195.71 ± 31.75
0.3	2.0	2.36 ± 0.44	320.72 ± 22.38	249.61 ± 25.06
0.3	2.4	1.80 ± 0.56	386.38 ± 28.48	337.56 ± 26.18
0.3	3.0	1.42 ± 0.45	471.69 ± 36.49	457.72 ± 36.17

for $Tt^{1/3}$ (42) and the entropy per particle S (44), to reach 90% of their maximum asymptotic value (see Figs. 8 and 9). One can then also extract the ''initial'' temperature and chemical potential that correspond to $t_{\rm eq}$ by using Eqs. (40)–(44).

The equilibration time $t_{\rm eq}$ is very sensitive to the values of α_S, c, and Q_s. Table I shows the equilibration time $t_{\rm eq}$, the initial temperature $T_{\rm eq}$, and the chemical potential μ for typical values of α_S, c, and Q_s. The parametric behavior of these quantities (for a fixed value of the nonperturbative constant c) as a function of Q_s, for two different values of the coupling constant α_S, is also shown in Fig. 10. Larger values of α_S and Q_s yield smaller $t_{\rm eq}$.

These results can be qualitatively understood as follows. One can show [see Eq. (37)] that the equilibration time is parametrically

$$t_{\rm eq}\sim\frac{1}{Q_s}\exp\left(\sqrt{\frac{2\pi}{c\alpha_S N_c}}\right).$$

In Fig. 10, we note that $t_{\rm eq}$ decreases roughly as $1/Q_s$. Also, it is greater for smaller α_S as one would expect from this expression. Similarly, from requiring that $tn(t)=$const, one finds for the initial temperature that

$$T\propto\frac{Q_s}{\alpha_S\exp\left(\sqrt{\frac{2\pi}{c\alpha_S N_c}}\right)}.$$

We see that this dependence on Q_s and α_S is confirmed in Fig. 10.

At RHIC, we expect (roughly) that $\alpha_S\sim0.3$, $c\sim1.3$, and $Q_s\sim$ 1.0 GeV. For the idealized initial conditions discussed here, the corresponding time and temperature at kinetic equilibrium are $t_{\rm eq}\sim3.2$ fm and $T_{\rm eq}\sim174$ MeV. At LHC, we expect $Q_s\sim$ 2–3 GeV, therefore $t_{\rm eq}\sim2.4-1.4$ fm and $T_{\rm eq}\sim321-472$ MeV. Are these numbers realistic? No (especially at RHIC), since it is unlikely that, at these temperatures, the system is a weakly coupled gluonic gas. At the time scales and temperatures corresponding to a rapid convergence of the system to the hydrodynamic limit, other (likely nonperturbative) effects might become important. One cannot conclude definitively that this is the case because we have not considered realistic initial distributions nor have we discussed the importance of particle number changing processes. We will comment on this point in the final section below.

VII. SUMMARY AND OUTLOOK

We have solved numerically a nonlinear transport equation, Eq. (22), which describes the evolution, after a heavy ion collision, of single particle gluon distributions in the central rapidity slice. The initial conditions for the solution of this equation are the highly anisotropic, idealized, initial con-

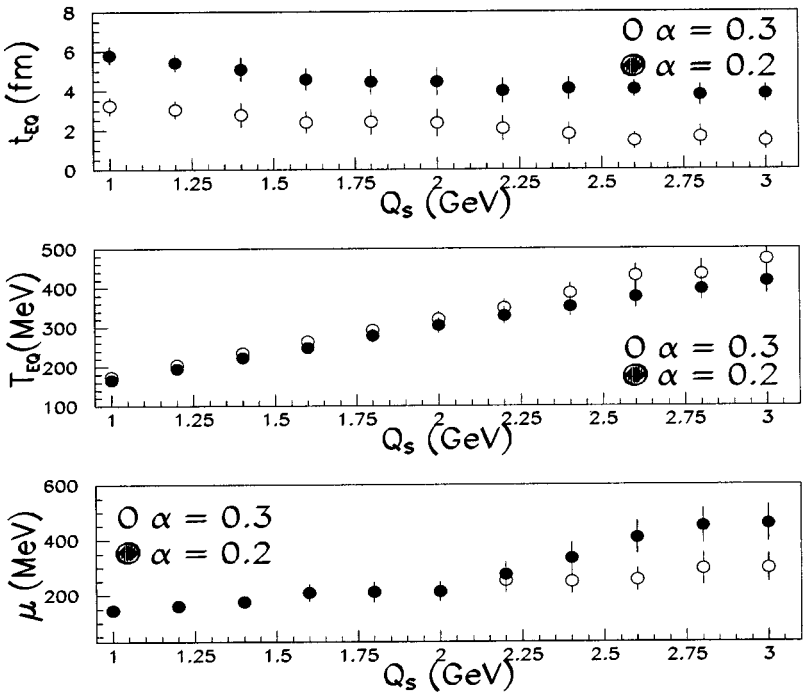

FIG. 10. The estimated values of the time $t_{\rm eq}$, temperature $T_{\rm eq}$, and the chemical potential μ, at the onset of equilibrium, plotted as functions of Q_s for $\alpha_S=0.2$ and 0.3.

ditions first discussed in the context of parton transport by Mueller [16,18]. The distributions are controlled by a single scale—the saturation scale Q_s of parton distributions in the nuclear wave function *before the collision*. Only elastic gluon-gluon scatterings are treated. Equilibration, in this approach, is dominated by small angle scattering. The collinear divergences that occur are regulated dynamically by a cutoff of the Debye form. We have checked that, at early times, the linearized Fokker-Planck equation reproduces the analytical results of Mueller. These analytical approximations however cannot be carried through to times relevant for equilibration.

We find that the tails of the initially highly anisotropic initial conditions converge very slowly to the expected isotropic equilibrium distribution. This behavior is confirmed by the behavior of $\langle p_z^2 \rangle$ and $\langle p_x^2 \rangle$. Despite the slow convergence of the single particle distributions to the isotropic thermal shape, thermodynamic observables such as the entropy per particle, the energy per particle, and the transverse and longitudinal pressures converge more rapidly to the hydrodynamic behavior expected of one-dimensional, boost invariant expansion. The more rapid convergence for these observables occurs because they are more sensitive to softer momentum modes and less so to the high momentum tails.

Using a particular criterion for equilibration (that thermodynamic observables have reached 90% of their asymptotic value), we extracted the equilibration times and the initial temperatures and chemical potentials. We have studied how they behave for varying values of Q_s and α_S. Even though small angle scattering is very inefficient (the equilibration time is an order of magnitude greater than the formation time), it is nevertheless smaller than the hydrodynamic time scale $t_{\rm hydro} \sim R/c_0$. Here R is the radius of the nucleus and c_0 is the speed of sound in the fluid. The relatively long equilibration times correspond to relatively low temperatures $T \ll Q_s$. At these temperatures, it is unlikely that the system can be described as a weakly coupled gluon gas. It is therefore reasonable to ask whether other effects, be they perturbative or nonperturbative in nature, may significantly alter our results.[11] We will enumerate below, in order of increasing complexity, those effects that are amenable to a weak coupling treatment.

First, recall that our results were obtained for idealized initial conditions. More realistic initial distributions have recently become available [15], and they are qualitatively different from the idealized distributions. Secondly, since the occupation numbers of the gluons are large initially, the effects of Bose enhancements in the Boltzmann equation should be taken into account. Both of these effects are straightforward to incorporate in our approach, and results with these improvements will be reported shortly [17].

Thirdly, as we discussed in the introduction, number changing $2 \to 3$ processes may be very important in establishing kinetic as well as chemical equilibrium [40]. Even though these processes are suppressed by an additional power of α_S, they are more efficient in redistributing the momenta [22]. Unfortunately, past treatments have been handicapped by uncertainties in how one treats infrared divergences. Work in progress suggests that this problem may be cured, and that equilibration is much more rapid [23]. If this is indeed the case, then initial temperatures are relatively close to the initial saturation scale, and the weak coupling treatment of equilibration will have been self-consistent.

Ultimately, the goal is relate the rich variety of hadronic and electromagnetic spectra that will soon be available at RHIC (and some years later, at LHC) to properties of the initial nuclear wavefunction, that may independently be probed in deeply inelastic eA or in pA collisions. This paper is a first quantitative step in that direction.

ACKNOWLEDGMENTS

We thank Jean-Paul Blaizot, Edmund Iancu, Keijo Kajantie, Alex Krasnitz, Dirk Rischke, Edward Shuryak, and Xin-Nian Wang for useful comments. In particular, we would like to thank Adrian Dumitru and Miklos Gyulassy on the one hand, and Al Mueller and Dam Son on the other, for illuminating discussions of their respective works in progress. Larry McLerran has provided wise comments and encouragement throughout the course of this work. This work was supported under U.S. DOE Contract Nos. DE-AC02-98CH10886 at BNL and DE-FG02-87ER40328 at the University of Minnesota.

APPENDIX: NUMERICAL ANALYSIS OF SECOND ORDER PARTIAL INTEGRODIFFERENTIAL EQUATIONS

Equation (22) is a second order partial integrodifferential equation whose numerical solution requires some care to ensure stability. Fortunately, standard finite differencing schemes can be used and numerical stability guaranteed. Equation (22) is of the form

$$\frac{\partial u}{\partial t} = A(t)\left(\frac{\partial^2 u}{\partial x^2} + \frac{\partial^2 u}{\partial y^2} + \frac{\partial^2 u}{\partial z^2}\right) + B(t)\left(\frac{\partial u}{\partial x} + \frac{\partial u}{\partial y} + \frac{\partial u}{\partial z}\right), \tag{A1}$$

where $u = u(t,x,y,z)$.

To discretize Eq. (A1) we first define a multidimensional grid

$$t = t_0 + n\Delta T, \quad x = x_0 + i\Delta, \quad y = y_0 + j\Delta, \quad z = z_0 + k\Delta,$$

where $n = 0,1,2,\ldots N$, $i = 0,1,2,\ldots I$, $j = 0,1,2,\ldots J$, and $k = 0,1,2,\ldots K$. Next we employ the alternating direction implicit (ADI) method using the crank-Nicholson finite differencing scheme [33]. The ADI method is especially useful in solving parabolic multidimensional equations on rectangular grids. For problems with three spatial dimensions, such as Eq. (A1), the ADI method is implemented by splitting each time step of size ΔT into three steps of size $\Delta T/3$. At the current fractional time step, $n + \frac{1}{3}$ for example, only one of the spatial derivatives are evaluated and the others are evaluated at the previous time step n. If we choose not to split the time step in such a way, the solution to Eq. (A1), after discretizing, would require us to invert a large matrix of the

[11] For an interesting recent take on this topic see Ref. [39].

same size as our grid. The purpose of splitting the time step in such a way is to reduce the problem in question into the solution of a tridiagonal matrix (as shown below). To illustrate this, Eq. (A1) is discretized using the ADI method with the crank-Nicholson finite differencing scheme. First discretize and evaluate the x derivatives at the current time step $n+\frac{1}{3}$:

$$\frac{u_{ijk}^{n+1/3}-u_{ijk}^{n}}{\Delta T/3}=\frac{A_n}{\Delta^2}[u_{i+1jk}^{n+1/3}+u_{i-1jk}^{n+1/3}-2u_{ijk}^{n+1/3}+u_{ij+1k}^{n}+u_{ij-1k}^{n}-2u_{ijk}^{n}+u_{ijk+1}^{n}+u_{ijk-1}^{n}-2u_{ijk}^{n}]+\text{linear terms}. \tag{A2}$$

Increment the time step by 1/3 and evaluate the y derivatives at current time step $n+\frac{2}{3}$:

$$\frac{u_{ijk}^{n+2/3}-u_{ijk}^{n+1/3}}{\Delta T/3}=\frac{A_n}{\Delta^2}[u_{i+1jk}^{n+1/3}+u_{i-1jk}^{n+1/3}-2u_{ijk}^{n+1/3}+u_{ij+1k}^{n+2/3}+u_{ij-1k}^{n+2/3}-2u_{ijk}^{n+2/3}+u_{ijk+1}^{n+1/3}+u_{ijk-1}^{n+1/3}-2u_{ijk}^{n+1/3}]+\text{ linear terms}. \tag{A3}$$

Increment the time step again by 1/3 and evaluate the z derivatives at the current time step $n+1$:

$$\frac{u_{ijk}^{n+1}-u_{ijk}^{n+2/3}}{\Delta T/3}=\frac{A_n}{\Delta^2}[u_{i+1jk}^{n+2/3}+u_{i-1jk}^{n+2/3}-2u_{ijk}^{n+2/3}+u_{ij+1k}^{n+2/3}+u_{ij-1k}^{n+2/3}-2u_{ijk}^{n+2/3}+u_{ijk+1}^{n+1}+u_{ijk-1}^{n+1}-2u_{ijk}^{n+1}]+\text{ linear terms}. \tag{A4}$$

In Eqs. (A2)–(A4), ''linear terms'' refers to the terms in Eq. (A1) which contain first order derivatives. Since the crank-Nicholson finite differencing scheme is stable only if the terms with the highest order of derivatives are implicit, the lower order terms are allowed to be either explicit or implicit. We assume here for brevity in notation that the linear terms are explicit and evaluated at the previous time step. Therefore, we do not write the linear terms out.

The solution to Eqs. (A2)–(A4) at every time step is simply the solution of a tridiagonal matrix at every n. For example, Eq. (A2) can be arranged as follows:

$$\alpha^n u_{i-1jk}^{n+1/3}+\beta^n u_{ijk}^{n+1/3}+\gamma^n u_{i+1jk}^{n+1/3}=\delta_{ijk}^{n}, \tag{A5}$$

where

$$\alpha^n=\gamma^n=-\frac{A_n\Delta T}{3\Delta^2},\quad \beta^n=2\frac{A_n\Delta T}{3\Delta^2},$$

and

$$\delta_{ijk}^{n}=\frac{A_n\Delta T}{3\Delta^2}[u_{ij+1k}^{n}+u_{ij-1k}^{n}-2u_{ijk}^{n}+u_{ijk+1}^{n}+u_{ijk-1}^{n}-2u_{ijk}^{n}]+\text{linear terms}.$$

Equation (A5) is simply an equation of the form

$$\mathbf{M}\cdot\mathbf{u}=\mathbf{d}, \tag{A6}$$

where $\mathbf{M}$ is a tridiagonal matrix. Since we know $\mathbf{M}$ and $\mathbf{d}$ at every previous time step n, we can in principal solve for $\mathbf{u}$ at every current time step $n+\frac{1}{3}$, given the boundary conditions u_{ijk}^{0}, u_{0jk}^{n}, u_{i0k}^{n}, and u_{ij0}^{n}. The inversion of sparse matrices (such as tridiagonal matrices) is usually numerically trivial.

In solving Eq. (A1) one needs to specify the boundary conditions suitable to solving a second order differential equation. In this work we have specified u_{ijk}^{0} by Eq. (3) and required that u vanish at the boundary of space u_{0jk}^{n}, u_{i0k}^{n}, u_{ij0}^{n}, u_{Ijk}^{n}, u_{iJk}^{n}, and $u_{ijK}^{n}=0$. Furthermore we require that the first derivatives vanish at $x,y,z\to\pm\infty$. Therefore, $u_{Ijk}^{n}-u_{I-1jk}^{n}\sim 0$, $u_{1jk}^{n}-u_{0jk}^{n}\sim 0$, and so on for j and k.

[1] K. Geiger, Phys. Rep. **258**, 237 (1995).

[2] K. J. Eskola, K. Kajantie, P. V. Ruuskanen, and K. Tuominen, Nucl. Phys. **B570**, 379 (2000).

[3] X. Wang, Phys. Rep. **280**, 287 (1997).

[4] L. McLerran and R. Venugopalan, Phys. Rev. D **49**, 2233 (1994); **49**, 3352 (1994); **50**, 2225 (1994).

[5] L. McLerran (private communication).

[6] R. V. Gavai and R. Venugopalan, Phys. Rev. D **54**, 5795 (1996).

[7] J. Jalilian-Marian, A. Kovner, L. McLerran, and H. Weigert, Phys. Rev. D **55**, 5414 (1997).

[8] Y. V. Kovchegov, Phys. Rev. D **54**, 5463 (1996).

[9] A. Ayala, J. Jalilian-Marian, L. McLerran, and R. Venugopalan, Phys. Rev. D **52**, 2935 (1995); **53**, 458 (1996).

[10] J. Jalilian-Marian, A. Kovner, L. McLerran, and H. Weigert, Phys. Rev. D **55**, 5414 (1997); J. Jalilian-Marian, A. Kovner, A. Leonidov, and H. Weigert, Nucl. Phys. **B504**, 415 (1997); J. Jalilian-Marian, A. Kovner, and Weigert, Phys. Rev. D **59**, 014015 (1999); L. McLerran and R. Venugopalan, *ibid.* **59**, 094002 (1999).

[11] A. Kovner, L. McLerran, and H. Weigert, Phys. Rev. D **52**, 6231 (1995); **52**, 3809 (1995).

[12] Y. V. Kovchegov and D. H. Rischke, Phys. Rev. C **56**, 1084 (1997); M. Gyulassy and L. McLerran, *ibid.* **56**, 2219 (1997); S. G. Matinyan, B. Müller, and D. H. Rischke, *ibid.* **56**, 2191 (1997); **57**, 1927 (1998); Xiao-feng Guo, Phys. Rev. D **59**, 094017 (1999).

[13] A. Krasnitz and R. Venugopalan, hep-ph/9706329; hep-ph/9808332; Nucl. Phys. **B557**, 237 (1999).

[14] A. Krasnitz and R. Venugopalan, Phys. Rev. Lett. **84**, 4309 (2000).

[15] A. Krasnitz and R. Venugopalan, hep-ph/0007108.

[16] A. H. Mueller, Nucl. Phys. **B572**, 227 (2000).

[17] J. Bjoraker and R. Venugopalan (in preparation).

[18] A. H. Mueller, Phys. Lett. B **475**, 220 (2000).
[19] E. M. Lifshitz and L. P Pitaevskii, *Physical Kinetics* (Pergamon Press, New York, 1981).
[20] R. Venugopalan, Acta Phys. Pol. B **30**, 3731 (1999).
[21] T. S. Biro, B. Müller, and X.-N. Wang, Phys. Lett. B **283**, 171 (1992); K. J. Eskola, B. Müller, and X.-N. Wang, *ibid.* **374**, 21 (1996); L. Kadanoff and G. Baym, *Quantum Statistical Mechanics: Green's Function Methods in Equilibrium and Nonequilibrium Problems* (Addison-Wesley, New York, 1989).
[22] S. M. H. Wong, Phys. Rev. C **54**, 2588 (1996).
[23] R. Baier, A. H. Mueller, D. Schiff, and D. T. Son, hep-ph/0009237; A. H. Mueller and D. T. Son (private communication).
[24] J. D. Bjorken, J. B. Kogut, and D. E. Soper, Phys. Rev. D **3**, 1382 (1971).
[25] J. D. Bjorken, Phys. Rev. D **27**, 140 (1983); K. Kajantie and L. D. McLerran, Nucl. Phys. **B214**, 261 (1983); G. Baym *et al.*, Nucl. Phys. **A407**, 541 (1983); M. Gyulassy and T. Matsui, Phys. Rev. D **29**, 419 (1984).
[26] G. Baym, Phys. Lett. **138B**, 19 (1984).
[27] S. Chapman and T. G. Cowling, *The Mathematical Theory of Nonuniform Gases* (Cambridge University Press, Cambridge, 1970).
[28] G. C. Nayak, A. Dumitru, L. McLerran, and W. Greiner, hep-ph/0001202; S. A. Bass and A. Dumitru, Phys. Rev. C **61**, 064909 (2000).
[29] G. Baym, H. Monien, C. J. Pethick, and D. G. Ravenhall, Phys. Rev. Lett. **64**, 1867 (1990).
[30] M. Le Bellac, *Thermal Field Theory* (Cambridge University Press, Cambridge, 1996).
[31] A. Selikhov and M. Gyulassy, Phys. Lett. B **316**, 373 (1993); H. Heiselberg, Phys. Rev. Lett. **72**, 3013 (1994); P. Arnold, D. T. Son, and L. G. Yaffe, Phys. Rev. D **59**, 105020 (1999); D. Bodeker, Phys. Lett. B **426**, 351 (1998).
[32] W. H. Press, B. P. Flannery, S. A. Teukolsky, and W. T. Vetterling, *Numerical Recipes* (Cambridge University Press, Cambridge, 1989).
[33] J. C. Strikwerda, *Finite Difference Schemes and Partial Differential Equations* (Wadsworth & Brooks, London, 1989).
[34] S. Gavin, Nucl. Phys. **B351**, 561 (1991).
[35] H. Heiselberg and X. N. Wang, Phys. Rev. C **53**, 1892 (1996).
[36] K. J. Eskola, K. Kajantie, and P. V. Ruuskanen, Nucl. Phys. **B323**, 37 (1989).
[37] M. Prakash, M. Prakash, R. Venugopalan, and G. Welke, Phys. Rep. **227**, 321 (1993).
[38] H. Heiselberg and X. N. Wang, Nucl. Phys. **B462**, 389 (1996).
[39] A. Dumitru and M. Gyulassy, Phys. Lett. B **494**, 215 (2000).
[40] T. S. Biro, E. van Doorn, B. Muller, M. H. Thoma, and X. N. Wang, Phys. Rev. C **48**, 1275 (1993); L. Xiong and E. Shuryak, *ibid.* **49**, 2203 (1994); D. M. Elliott and D. H. Rischke, Nucl. Phys. **A671**, 583 (2000).